CME SAM

Musculoskeletal Imaging

AJR FOCUS ON:

MRI of Spinal Bone Marrow: Part 1, Techniques and Normal Age-Related Appearances

Lubdha M. Shah[1]
Christopher J. Hanrahan

OBJECTIVE. This article reviews MRI protocols, including routine and nonroutine pulse sequences as well as the normal MRI appearance of spinal marrow and expected age-related changes.

CONCLUSION. Routine MRI of the spine provides useful evaluation of the spinal bone marrow, but nonroutine MRI pulse sequences are increasingly being used to evaluate bone marrow pathology. An understanding of MRI pulse sequences and the normal and age-related appearances of bone marrow is important for the practicing radiologist.

The MRI appearance of the bone marrow is determined by the relative amount of protein, water, fat, and cells within the marrow and depends on the pulse sequence on which it is being evaluated. The major determinants of the MR appearance of bone marrow are the fat and water content. The routine spine evaluation on MRI typically includes T1-weighted, T2-weighted, and STIR sequences. The next sections will discuss these sequences, including the bone marrow appearance on each as well as the utility of other nonroutine sequences in evaluating bone marrow in a problem-solving capacity.

Routine Sequences

T1-Weighted Imaging

T1-weighted spin-echo (SE) images are best to evaluate the cellular content in bone marrow because of high fat content interspersed with hematopoietic elements. The hydrophobic carbon-hydrogen groups in fat result in a short T1 relaxation time because of very efficient spin-lattice relaxation [1]; conversely, water has a long T1 relaxation time [2]. Yellow marrow has signal intensity (SI) comparable with subcutaneous fat, whereas red marrow has intermediate T1 relaxation with SI lower than subcutaneous fat but higher than disk or muscle [2] (Fig. 1). The exact SI of the marrow, however, is dependent on the proportion of red and yellow marrow. Cellular infiltration retains some intermixed fat, whereas replacement obliterates all fat within the bone marrow [3]. This replacement of the bone marrow characteristically appears hypointense relative to disk and muscle on T1-weighted images [3] and hypointense relative to normal marrow [4, 5]. Marrow T1-weighted hypointensity, however, is nonspecific. Generally, bone marrow signal that is hypointense to adjacent muscle or intervertebral disk at 1.5 T is abnormal with accuracy of 94% and 98%, respectively [6]. At 3-T field strength, Zhao et al. [7] showed a higher diagnostic accuracy comparing T1 marrow SI to muscle (89%) rather than disk (78%). For focal abnormalities, the bull's-eye sign (i.e., a focus of high T1 signal intensity in the center of an osseous lesion) has been reported to be a specific indicator of normal hematopoietic marrow (sensitivity, 95%; specificity, 99.5%) [8] (Fig. 2). With diffuse abnormalities, extensive replacement of the vertebral bone marrow may initially create the impression of a normal study because of its homogeneity, and careful comparison of T1-weighted marrow signal to disk or muscle is required to make the diagnosis (Fig. 3).

T2-Weighted Imaging

Conventional T2-weighted sequences can also be helpful for evaluating bone marrow pathology. Fat protons have a relatively long T2 relaxation because of less-efficient spin-spin relaxation [1]. Yellow marrow shows intermediate and high SI on T2-weighted SE and T2-weighted fast SE (FSE) MRI, respectively. Fatty marrow appears higher in SI than muscle and equal to or slightly lower in

Keywords: bone marrow, MRI, spine protocol

DOI:10.2214/AJR.11.7005

Received March 27, 2011; accepted after revision June 27, 2011.

Presented at the 2010 annual meeting of the American Roentgen Ray Society, San Diego, CA.

[1]Both authors: Department of Radiology, University of Utah School of Medicine, 30 North 1900 East #1A71, Salt Lake City, Utah 84132. Address correspondence to C. J. Hanrahan (christopher.hanrahan@hsc.utah.edu).

CME/SAM
This article is available for CME/SAM credit.
See www.arrs.org for more information.

AJR 2011; 197:1298–1308

0361–803X/11/1976–1298

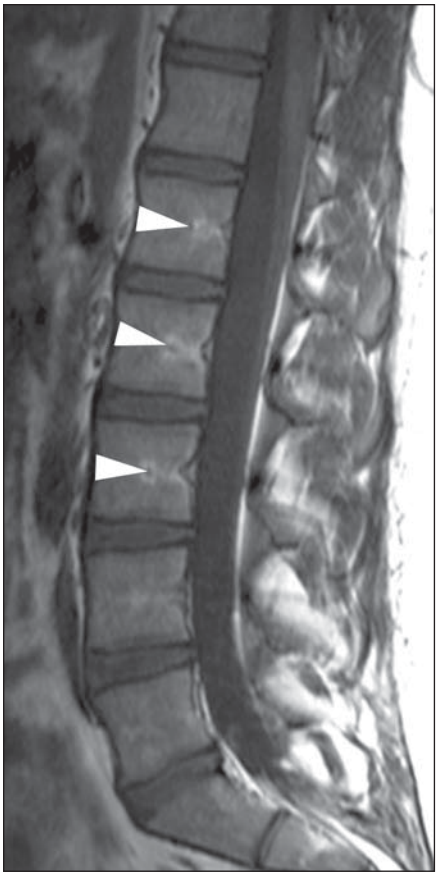

Fig. 1—28-year-old man with vague back pain. Sagittal T1-weighted spin-echo image shows normal marrow signal intensity of lumbar vertebral bodies, which are slightly hyperintense relative to adjacent intervertebral disks. White arrowheads depict normal fat signal intensity in region of basivertebral plexus.

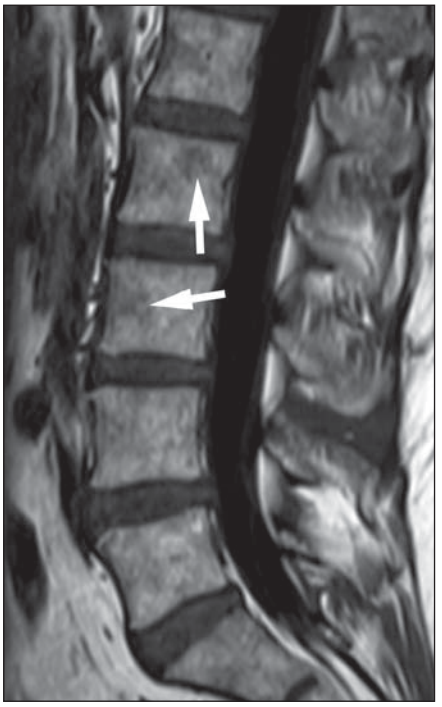

Fig. 2—64-year-old woman with chronic low back pain. Central hyperintense signal (*arrows*) is seen within vague hypointense lesions within L2 and L3 vertebral bodies on this sagittal T1-weighted image, consistent with bull's eye sign of normal hematopoietic marrow. Overall heterogeneous appearance of marrow is due to osteoporosis.

Fig. 3—58-year-old woman with breast cancer. Sagittal T1-weighted image of thoracic spine illustrates diffuse marrow hypointensity, which is slightly hypointense relative to disks. Given diffuse marrow involvement, it may be difficult to discern this marrow abnormality.

SI than subcutaneous fat. Because water and fat are closer in SI, there is decreased contrast of the spinal marrow on this sequence. Moreover, FSE sequences do not fully suppress fat signal such that the contrast differences between red and yellow marrow can be difficult to delineate. Red marrow SI is slightly lower than that of yellow marrow [9]. Although metastatic lesions are usually brighter than normal bone marrow on T2-weighted MRI due to their high water content, they sometimes can be difficult to differentiate from normal marrow on T2-weighted sequences [10]. The halo sign, characterized by a rim of bright T2 signal, sometimes may be detected on T2-weighted MRI and indicates the presence of malignancy [8] (Fig. 4). Schweitzer et al. [8] showed high specificity of both the halo sign and diffuse T2-weighted signal hyperintensity for metastatic disease (sensitivity, 75%; specificity, 99.5%) [8]. Both conventional SE and FSE T2-weighted sequences have been shown to detect the same number of bone marrow lesions [11]. The rapidity of the FSE T2-weighted sequence has made it the more common T2-weighted sequence used for clinical imaging.

Fat Saturation

As a part of the routine MR sequences, the combination of T1-weighted and either fat-saturation T2-weighted or STIR images is highly effective for the evaluation of bone marrow lesions [10]. Bone marrow contrast can be accentuated by using fat-suppressed sequences, either the chemically selective fat-saturation technique or STIR images (discussed later) [12]. Fat saturation can be applied to T2-weighted and gadolinium-enhanced T1-weighted images. At 1.5 T, a 210-Hz difference exists between the resonant frequency of fat and water [13]. For these sequences, a selective radiofrequency saturation pulse and dephasing gradient is applied based on the 210-Hz chemical shift, which suppresses the lipid signal but only minimally affects the signal coming from nonlipid tissues, such as water [13]. This narrow saturation band requires a very homogeneous magnetic field and is sensitive to magnetic field inhomogeneities from susceptibility differences, such as off-isocenter imaging and a large FOV. Poor fat saturation can be problematic, particularly when evaluating bony edema on T2-weighted and osseous lesions on contrast-enhanced T1-weighted images (Fig. 5). Additionally, orthopedic implants may result in poor fat saturation because of local magnetic field inhomogeneity. This may be secondary to shifting of the resonant frequencies of water and fat, prevention of the frequency-specific saturation pulse from targeting fat, or unintended suppression of water signal [13] (Fig. 6).

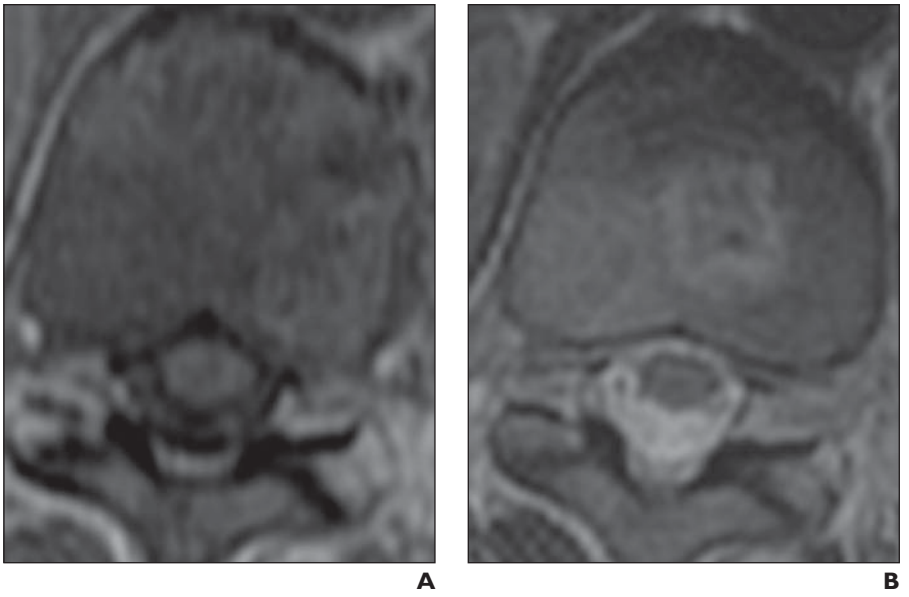

Fig. 4—Halo sign.
A and **B,** Axial MR images in 25-year-old woman who presented with radiculopathy and was found to have metastatic synovial sarcoma show low T1-weighted signal and peripheral rim of increased T2-weighted signal within T11 metastatic lesion.

Techniques such as increasing the bandwidth and orienting the frequency encoding direction parallel to the hardware can reduce related susceptibility artifact.

With the addition of fat-suppression techniques, bone marrow SI may be altered. On fat-saturated T2-weighted MRI, hematopoietic marrow shows intermediate SI similar to that of muscle, whereas fatty marrow shows SI lower than that of muscle. By comparison, most marrow pathology exhibits relatively high SI, greater than that of red and yellow marrow, on fat-suppressed images. Uchida et al. [14] studied 22 patients, comparing nonneoplastic and metastatic bone marrow using T1-weighted SE and chemical shift fat-saturated T1-weighted imaging. On fat-saturated T1-weighted images, they found that metastases show mixed to high SI, whereas nonneoplastic lesions have low SI.

STIR Imaging

The STIR sequence provides high tissue contrast, which is useful in evaluating bone marrow (Fig. 7). The differences in longitudinal relaxation between fat and water protons result in differences in the T1 relaxation, which are the basis of the STIR technique [15]. An inversion time (TI) is chosen at the time to null the signal generated by fat. First, a nonselective 180° radiofrequency inversion pulse is applied. This is followed by a second 90° pulse, which is applied at the TI, which is the time the previously inverted longitudinal magnetization of fat crosses the null point [14, 15]. With this series of pulses, the signal from fat is suppressed and the signal from water is preserved in the selected slice.

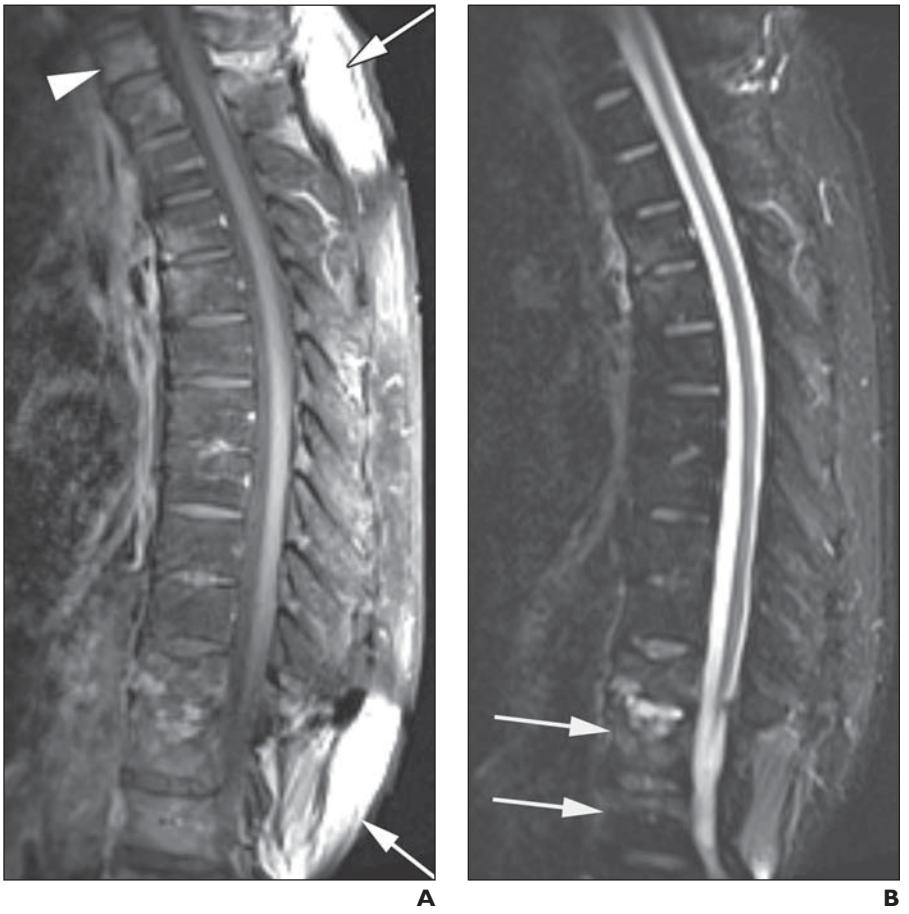

Fig. 5—61-year-old woman with mid thoracic pain.
A, Magnetic field distortion at superior and inferior aspects of thoracic spine (*arrows*) results in poor fat saturation on this sagittal T1-weighted contrast-enhanced MR image with fat saturation. This artifact creates false-positive "enhancement" in upper thoracic vertebral bodies (*arrowhead*).
B, STIR image displays no abnormal signal intensity in upper thoracic vertebral bodies to suggest edema related to marrow process. Edema and superior endplate deformities of lower thoracic vertebral bodies (*arrows*) are compatible with acute compression fractures.

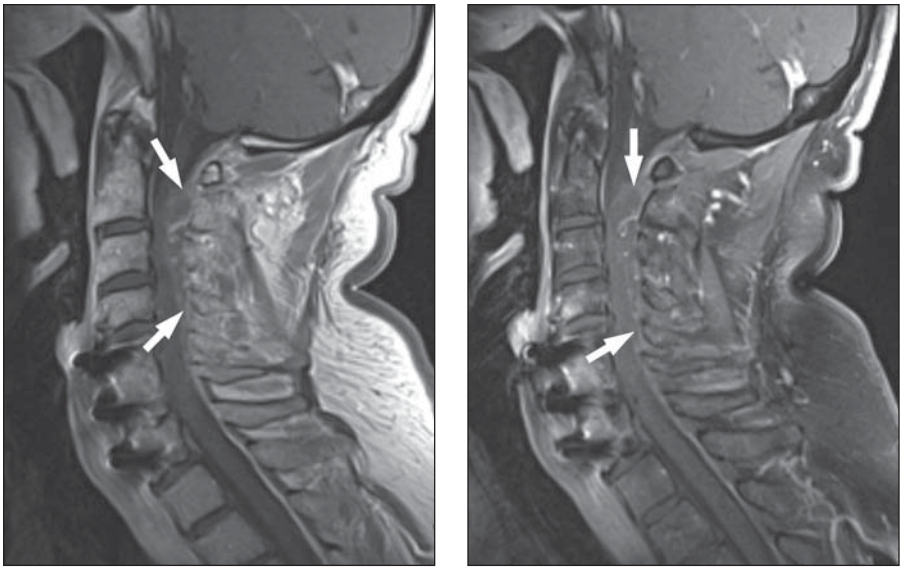

Fig. 6—45-year-old man with neck pain.
A and **B,** Sagittal T1-weighted contrast-enhanced MR images without (**A**) and with (**B**) fat saturation depict C5–C7 anterior cervical diskectomy and fusion with vertebral body screws. Assessment of marrow at fused levels is significantly limited because of hardware-related magnetic susceptibility artifact. There is heterogeneously enhancing hematoma in dorsal epidural space (*arrows*).

The STIR sequence tends to produce more homogeneous fat suppression than T2-weighted FSE, which is performed with frequency-selective fat saturation. The main drawback of the STIR sequence is that it cancels every signal close to fat [15]. Troublesome examples of this include tissue that enhances with contrast administration (e.g., if STIR is performed after contrast administration) and blood products in a hematoma. Although the conspicuity of lesions is similar on STIR and fat-saturated T2-weighted imaging, the latter has several practical advantages, including acquisition of more slices per unit of time and improved tissue specificity [10]. Although the STIR sequence is time consuming, with only a limited number of slices acquired at one time, this can be overcome by using fast STIR sequences [16].

Gadolinium-Enhanced T1-Weighted Imaging

Gadolinium-enhanced T1-weighted images may be helpful in detecting some marrow lesions; however, enhancing lesions may be difficult to discern if they become isointense to normal bone marrow (Fig. 8). Sequences that suppress the SI of normal fatty bone marrow allow better identification of the enhancing metastatic foci [17, 18]. However, Meyer et al. [19] showed, in their study of 91 patients with neuroblastoma being evaluated for bone marrow metastases, that although the conspicuity of lesions was increased with the heterogeneous pattern of enhancement on gadolinium-enhanced T1-weighted images with fat saturation, the sensitivity of lesion detection was not increased. On the other hand, contrast administration can be helpful in confirming malignancy or osteomyelitis and evaluating the extent of extramedullary spread [20]. In

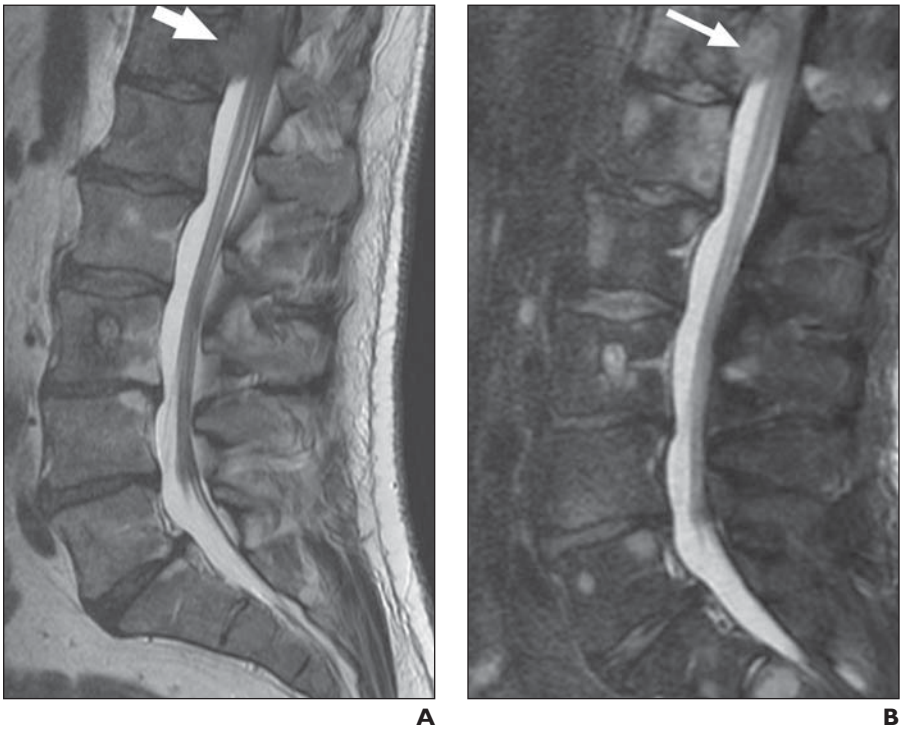

Fig. 7—51-year-old woman with metastatic breast cancer.
A, Sagittal fast spin-echo T2-weighted MR image illustrates few heterogeneously hypointense metastatic lesions in lumbar spine. In particular, T12 lesion has epidural component compressing conus medullaris (*arrow*).
B, Sagittal STIR MR image shows increased conspicuity of numerous hyperintense metastatic lesions in lumbar spine and sacrum, including T12 lesion compressing conus medullaris (*arrow*).

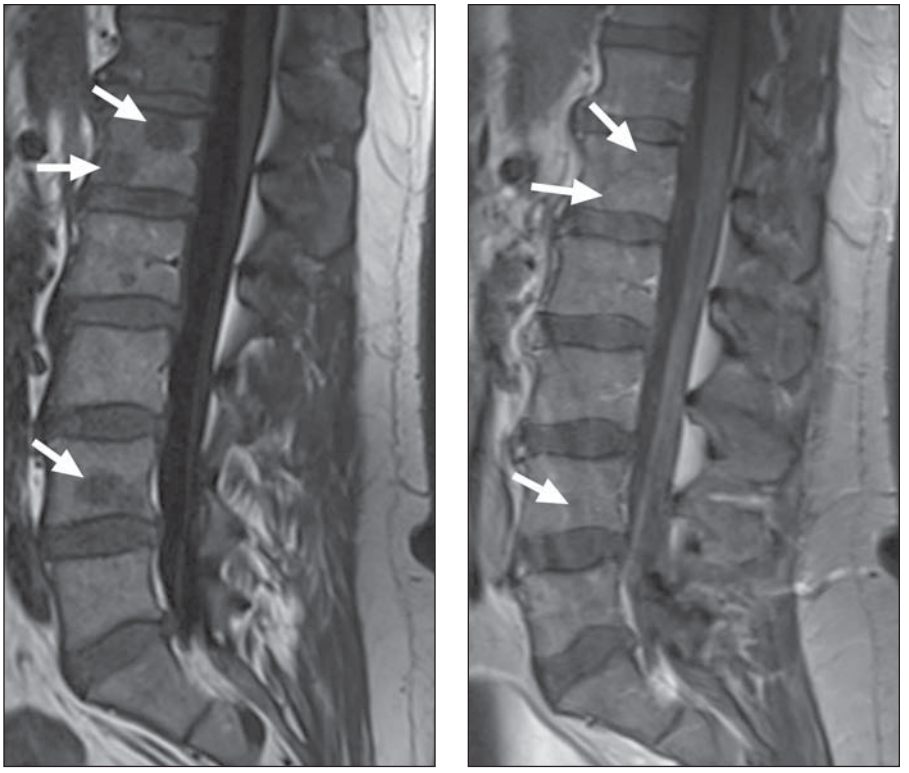

Fig. 8—45-year-old man with systemic sarcoidosis, including osseous involvement.
A, Multiple round hypointense lesions (*arrows*) are detected on sagittal T1-weighted image, compatible with mixed lytic-sclerotic osseous lesions of sarcoidosis.
B, Sagittal T1-weighted contrast-enhanced MR image illustrates difficulty of lesion detection within marrow on enhanced sequences without fat saturation. Vague enhancing foci (*arrows*) are compatible with mixed lytic-sclerotic osseous lesions of sarcoidosis.

addition, contrast administration allows identification of lesions that may alter treatment, particularly lesions that spread to the epidural space and may result in compression of the spinal cord [21].

Nonroutine Sequences

Several nonroutine MRI sequences can be used to obtain additional information about spinal bone marrow. Diffusion-weighted imaging (DWI), in- and out-of-phase MRI, MR spectroscopy (MRS), and dynamic contrast-enhanced MRI (DCE-MRI) aim to increase contrast and visualize changes in the bone marrow at a molecular level.

T1 FLAIR Imaging

The T1 FLAIR sequence is proving to be a useful sequence in spinal imaging (Fig. 9). FLAIR techniques typically use long TE readout (increased T2-weighting) to null CSF signal and thereby improve the conspicuity of tissue abnormalities without the diagnostically problematic effects of CSF pulsation artifacts and volume averaging [22–25]. Rapid acquisition with relaxation enhancement (RARE) techniques, which are equivalent to FSE, can be incorporated with basic FLAIR sequences to improve the efficiency [26]. With this imaging technique, a fast T1-weighted inversion recovery sequence with different TI pairs to null CSF and vary T1 effects on non-CSF tissues is coupled to a RARE readout [27]. This sequence is also particularly useful with 3-T MRI because there is decreased fluid contrast that is associated with the lengthened T1 relaxation times seen with higher magnetic strength [25]. In addition to evaluating spinal cord pathology, Melhem et al. [28] have shown that the T1 FLAIR sequence optimizes the tissue contrast between fatty marrow and abnormal tissue. Thus, there is improved conspicuity of edema and metastatic lesions in the bone marrow. Recent literature has also shown that the T1 FLAIR sequence is sensitive for detecting bone marrow pathology [29].

Diffusion-Weighted Imaging

DWI evaluates the tissue-specific molecular diffusion of protons, which may be useful in differentiating bone marrow pathology. For example, in tissues with high cell densities (such as with neoplasm), a decreased apparent diffusion coefficient (ADC) is expected because the exaggerated amount of intra- and intercellular membranes results in restricted diffusion. However, the utility of DWI on differentiating benign from metastatic spinal lesions is controversial. One study using DWI found all benign vertebral compression fractures to be hypo- to isointense compared with adjacent normal vertebral bone marrow, whereas pathologic compression fractures were hyperintense [5]. This study found a statistically significant difference ($p < 0.001$) between the calculated contrast ratios comparing benign and pathologic vertebral fractures [5]. In contrast, Castillo et al. [30] evaluated 15 patients with metastases and showed that DWI of the spine offered no advantage in the detection and characterization of vertebral metastases compared with unenhanced T1-weighted imaging. Nevertheless, they did conclude that DWI was superior to T2-weighted imaging in detecting malignant lesions [30]. Others have shown that, rather than qualitative assessment, the quantitative evaluation of the ADC in vertebral bodies may be useful for differentiating malignant from benign vertebral tissue [31]. In their small study of eight patients with epidural metastatic disease, Plank et al. [32] concluded that DWI may be a useful technique for the evaluation of epidural lesions causing spinal cord compression. They showed decreased diffusivity in neoplastic lesions with higher cellularity [32].

In addition to tumor evaluation, DWI may be useful for differentiation of degenerative and infectious endplate abnormalities. In a recent study of 16 patients with endplate ab-

Fig. 9—72-year-old man with acute perineal anesthesia superimposed on chronic low back pain. Sagittal T1-weighted inversion recovery image exhibits discrete delineation of disk protrusions from CSF (*arrowheads*). T1-weighted inversion recovery sequence also better demarcates compression of cauda equina by disk protrusion at L2–L3 (*arrow*).

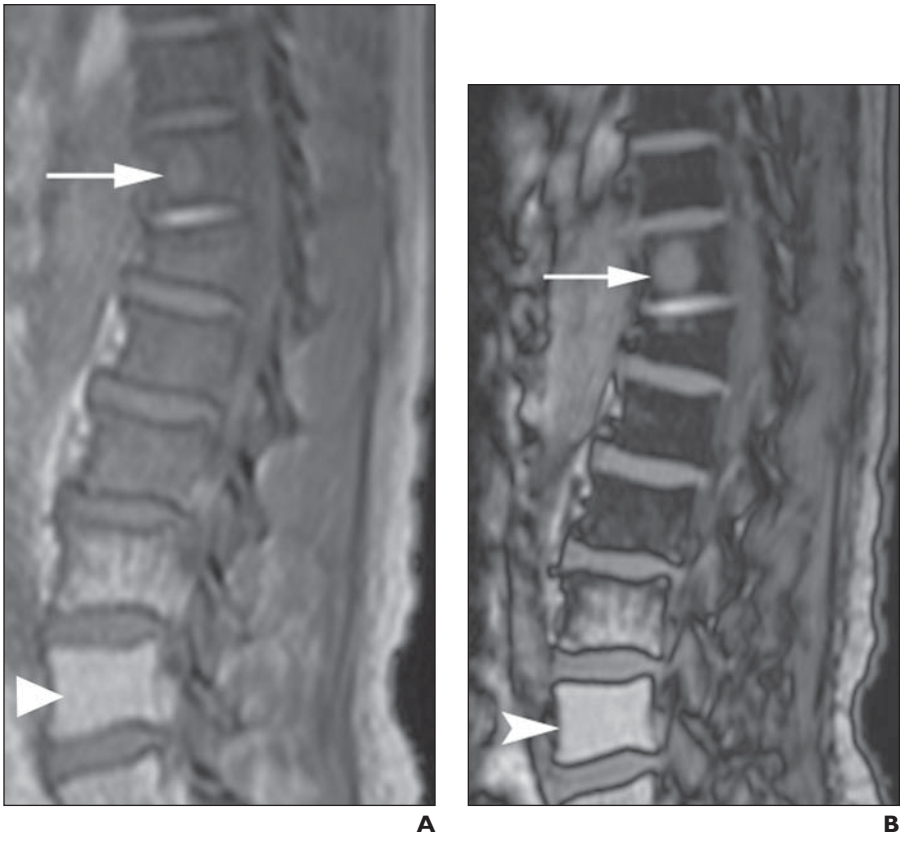

Fig. 10—68-year-old man with multiple myeloma.
A, Sagittal T1-weighted in-phase image shows abnormal marrow signal in T11 vertebral body (*arrow*) due to myeloma lesion. Lower lumbar vertebral bodies show fat marrow replacement due to radiation therapy (*arrowhead*) and therefore remain hyperintense on both in- and out-of-phase images.
B, Sagittal T1-weighted out-of-phase image shows abnormal hyperintense marrow signal in T11 vertebral body (*arrow*) due to myeloma lesion. Vertebral bodies with normal marrow show dark signal intensity. Lower lumbar vertebral bodies show fat marrow replacement (*arrowhead*) and therefore remain hyperintense on both in- and out-of-phase images.

Fig. 11—38-year-old woman with low back pain.
A, Sagittal T1-weighted spin-echo image obtained using 1.5-T MRI scanner depicts normal marrow hyperintense signal intensity relative to intervertebral disks.
B, Sagittal T1-weighted spin-echo image obtained using 3-T MRI scanner approximately 3 years after initial scan shows reduced contrast resolution on standard T1-weighted spin-echo images. Increased susceptibility effects from trabeculae result in lower signal intensity of bone marrow.

normalities, DWI showed hyperintensity in five patients with infection and no hyperintensity in 11 patients with degenerative endplate changes, seven of which were classified as Modic type 1 [33]. ADC values of infectious endplates were significantly higher than normal and degenerative endplates [33].

DWI also may prove useful in distinguishing progressive changes in bone marrow among treatment sequelae, fracture, or tumor, which can be difficult on conventional MRI. In one study, Hanna et al. [34] compared MRI scans using T1-weighted, T2-weighted, STIR, and contrast-enhanced T1-weighted sequences with histologic specimens at 21 sites, 7 of which contained tumor and 14 of which were tumor-free. For all of the tumor-positive sites, the MRI scans revealed abnormalities. For the sites without tumor, there was a significant (more than 50%, depending on the pulse sequence) false-positive rate, presumably because tumor could not be distinguished from the effects of treatment [34]. However, DWI sequences may show decreased SI of metastatic disease of the vertebral marrow with successful treatment [35]. In a study of 24 patients with metastatic disease of the spine, Byun et al. [35] showed decreased DWI signal of the spine greater than 1 month after therapy in patients with clinical improvement, whereas persistently abnormal hyperintense signal was found when there was no clinical improvement.

Chemical Shift Imaging

Chemical shift, or in- and out-of-phase, imaging may be useful in detecting pathology because it takes advantage of the difference in resonance frequency between fat and water protons, which are abundant in bone marrow. Water and fat protons are in phase with one another at a TE of 4.6 milliseconds and 180° opposed at a TE of 2.4 milliseconds at 1.5 T. When a given voxel contains both fat and water, there will be some SI loss on images that are obtained when the protons are in their opposed phase (TE 2.4 milliseconds). More SI suppression occurs when the volume of fat and water is roughly equal. The presence of both fat and water in normal marrow results in suppression of SI on opposed-phase images [36, 37]. An early study by Wismer et al., [38] showed that hematopoietic marrow yields low SI on out-of-phase images and pathologic conditions in red marrow typically result in increased SI because of higher proportions of lipid or water. On the other hand, because of its high fat content, yellow marrow normally yields high SI on out-of-phase images. Pathologic conditions in yellow marrow exhibit decreased SI because of increased tissue water due to the combination of accumulated tissue water and the normally high fat content in these sites [38]. Red marrow reconversion will display normal low signal on out-of-phase imaging because both fat and water elements are present [39].

In- and out-of-phase imaging can be used to determine whether a signal abnormality in bone marrow is due to a neoplastic process [40]. Neoplastic conditions replacing normal marrow will not have signal dropout on out-of-phase images (Fig. 10). In their study of 30 patients, Disler et al. [40] calculated relative SI ratios to predict whether lesions were neoplastic or nonneoplastic, and using a 0.81 cutoff value, they achieved sensitivity and specificity of 95%. This technique has also been used to differentiate acute benign versus malignant vertebral fractures [41]. In benign compression fractures, although conventional SE sequences reveal abnormal SI, no marrow-replacing process has occurred. This normal marrow fat results in suppression of SI on opposed-phase images. In pathologic fractures, normal fat-containing marrow is replaced with tumor, which results in lack of suppression on the opposed-phase images. Studies have found a difference in the SI ratio between benign and pathologic compression fractures (sensitivity, 0.95; specificity, 1–0.8) [41, 42].

There are pitfalls to consider in chemical shift imaging, Radiation therapy may normalize the signal-to-noise ratio in treated lesions [41], whereas marrow fibrosis may result in a false-positive interpretation. Susceptibility artifact associated with sclerotic metastases and fracture-related hematoma

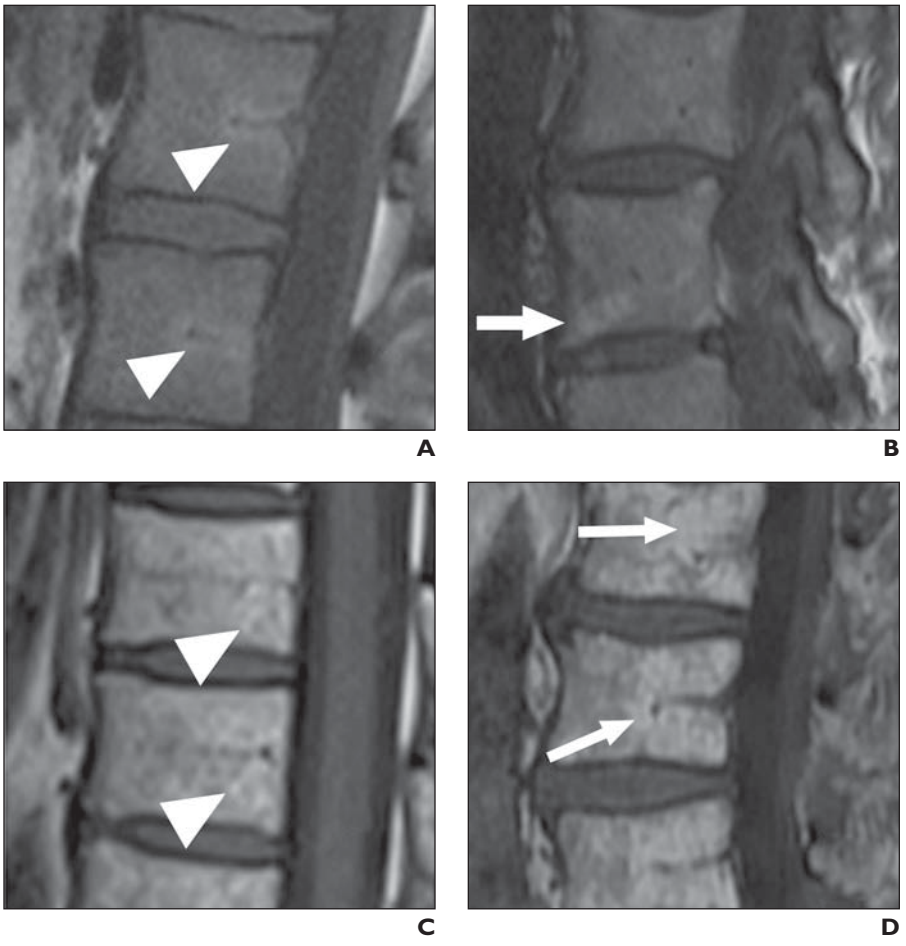

Fig. 12—Examples show normal age-age related T1-weighted appearance of spinal bone marrow. **A–D,** T1-weighted images of lumbar (**A, B,** and **D**) and thoracic (**C**) spine show common appearances of bone marrow. Spinal bone marrow of patients younger than age 40 years typically has fat adjacent to basivertebral vein (*arrowheads*, **A**). Patients older than 40 years can have peripheral bandlike fatty deposits (*arrow*, **B**), multiple (sometimes confluent) small foci of fat (*arrowheads*, **C**), or multiple large foci of fat (*arrows*, **D**).

may result in a false-positive result [39]. On the other hand, metastases containing fat, such as renal cell carcinoma and infiltrative multiple myeloma, may result in a false-negative interpretation [39]. In such cases, histopathologic confirmation may be needed.

Dynamic Contrast-Enhanced MRI

Studies have shown an increase in SI within the bone marrow of healthy individuals after gadolinium administration because of bone vascularity [43, 44]. Montazel et al. [45] showed that normal spinal marrow DCE-MRI patterns are dependent on age and fat content [45]. Furthermore, younger subjects may exhibit a percentage of SI increase within the range typical of diffuse malignant marrow infiltration [44]. Higher perfusion parameters are noted in hematopoietic marrow, which is characterized by numerous fenestrated vessels, large vascular pools and channels, and small amounts of poorly vascularized fat [2]. Bone marrow enhancement decreases markedly with increasing age and conversion to fat, although there is significant variability among subjects [45]. This difference in fat composition of bone marrow may be responsible for the interindividual differences in SI after contrast enhancement [44]. Arteriosclerosis associated with aging may alter marrow perfusion and result in ischemic change [46]. Chen et al. [46] showed decreased perfusion in both sexes with increasing age, more marked in women. Studies have also shown a reduction in perfusion indexes within the vertebral body and paraspinal tissues supplied by the same artery as the bone mineral density decreases in both genders [47, 48].

DCE-MRI of bone marrow has been used in patients with lymphoproliferative disease and diffuse marrow infiltration as well as in the assessment of response to chemotherapy [49–51]. The percentage of SI increase has been seen in intermediate-grade and high-grade diffuse marrow infiltration compared with healthy subjects [44]. This MR technique has also been applied in predicting the progression of collapse of an osteoporotic vertebral fracture. Kanchiku et al. [52] found an increased tendency of progression of vertebral collapse with increased unenhanced areas on DCE-MRI.

Proton MR Spectroscopy

In addition to DWI, proton MRS [53] has been used in assessing bone marrow changes with varying bone mineral densities. Proton MRS allows the noninvasive quantitative assessment of bone constituents, particularly fat, at the molecular level [54, 55]. In this technique, the global MR signal from bone is divided into the two major segments of water and lipid separated by 3.1 ppm. The spectra of proton MRS have a water peak, originating mostly from red marrow, and a lipid peak, arising from yellow marrow [2, 56]. The lipid signal is composed of at least eight fractions [57], the largest of which is from the methylene group at 1.6 ppm. Signal peaks can vary among subjects and are influenced not only by the water-lipid proton quantity and the tissue environment but also by the surface coil and the distance between the voxel and surface coil [58]. Because of these variables, instead of measuring the absolute signal peak for signal quantification, a lipid-water ratio is often measured [58]. The fat fraction value determined from MRS has been adopted as a predictor of bone marrow fat content in most studies [47, 58].

MRS has been used to illustrate the increase in fat content with age [59]. Demmler et al. [60] showed that a decrease in cancellous bone was accompanied by a corresponding increase in fat cells and decrease in arterial capillaries and sinuses in bone marrow. Not only has it been shown that vertebral marrow fat increases as bone marrow density decreases [47, 48], but also inferences of osseous quality may be made. In a study of 22 patients, Schellinger et al. [58] used proton MRS to show that the percentage fat fraction was higher in lumbar vertebral bodies of subjects with weakened bone compared with the control group, suggesting it could serve as a measure of bone quality. Because the density and spatial orientation of the trabeculae influence the microscopic homogeneity of the magnetic field inside the marrow [55], the line width may be used to reflect bone density. Increased bone density will cause greater magnetic field inhomogeneity and wider spectral peaks as opposed to narrow peaks due to decreased bone mineral density [58].

As stated previously, MR diffusion techniques depend primarily on the interstitial fluid flow, cellularity, and extracellular water volume and, to a lesser extent, on microvascular perfusion [61]. Increased interstitial fluid flow along bone canaliculi from repeated mechanical deformation has been proposed as an explanation for the anabolic adaptive responses to mechanical stress occurring within bone. Although Griffith et al. [47] found no relationship between bone marrow ADC and bone density, Liu et al. [62] showed a positive correlation between ADC and bone mineral density. Griffth et al. did find a weak negative association between marrow ADC and marrow fat content, indicating a reduction in molecular diffusion as marrow fat content increased. Similarly, ADC has been shown to correlate negatively to fat fraction values of vertebral bodies [62], which is due to the increased fat packing of bone marrow taking place in the dilated intertrabecular space because of osteoporosis.

Fig. 13—28-year-old pregnant woman with right upper extremity and neck pain after fall. Sagittal T1-weighted MR image reveals diffuse marrow hypointensity, which remains isointense to muscle. This signal intensity is due to red marrow recruitment in setting of rapid red cell turnover.

3-T MRI

Higher-magnetic-field-strength MRI has the advantage of increased signal-to-noise ratio, which can be used to improve contrast and spatial resolution [63]. Another advantage is that the more rapid scanning time is associated with reduced patient motion artifacts. However, higher magnetic field strengths are associated with particular challenges, and the sequence parameters have to be adjusted. The increased T1 relaxation time with increased magnetic field strength can result in reduced contrast resolution on standard T1-weighted SE images, although there may be improved background suppression on MR angiography. Increased susceptibility effects from trabeculae result in lower SI of bone marrow [64] (Fig. 11). The transverse relaxation may have to be increased on FSE sequences. Other modifications for higher field strength include maximizing echo-train length and decreasing slice thick-

ness and time to echo. The latter is necessary to achieve contrast resolution on T2-weighted imaging because of the reduced T2/T2* relaxation times [24].

The increased effects of magnetic susceptibility can result in signal loss in regions of greater signal dephasing on T2-weighted MRI, such as at tissue-bone and tissue-air interfaces. Increasing the spatial resolution with thinner slices or using parallel imaging may help minimize these magnetic susceptibility effects [24]. With higher magnetic field strength, there is a proportional increase in chemical shift artifact. This spatial misregistration of fat tissue relative to water tissue in the frequency-encoding direction degrades standard SE images [24]. Modifications such as increasing bandwidth can reduce chemical shift artifact but result in decreased signal-to-noise ratio.

Another important consideration is the potentially increased energy deposition in the patient and hardware with higher field strengths. The rate of radiofrequency-induced heat deposited in the patient is increased. This increased specific absorption can be managed by reducing the acquisition flip angle and decreasing the number of phase encoding steps.

Age-Related Changes of Spinal Marrow by T1-Weighted MRI

To identify abnormal bone marrow on imaging, an understanding of the normal pattern of bone marrow maturation that occurs with age is important. The developmental maturation occurs through the replacement of active hematopoietic marrow, which is actively producing mature blood cells from progenitors, by primarily fatty marrow that no longer produces hematopoietic cells [2]. Humans are born with nearly their entire skeleton composed of red marrow, which converts to fatty marrow over time in an organized predictable fashion. This proceeds in a distal to proximal manner until the age of 25 years when the adult pattern of marrow is in place, with the axial and proximal appendicular skeleton containing the remaining red marrow [2].

MRI of bone marrow has a variable appearance because of the age-related distribution of cellular and fatty marrow. These patterns have large interindividual variations among healthy subjects of a given age. In contrast, marrow distribution and SI patterns show little variation among each vertebral body of the same subject [65]. In addition, the normal distribution patterns of cellular and fatty marrow can be difficult to distinguish from focal or diffuse marrow infiltration [3, 66, 67]. For example, the SI of hematopoietic marrow in neonates may be slightly lower than that of muscle on T1-weighted MRI, reflecting the larger percentage of cellular marrow. Subsequent to the neonate period, however, the SI of bone marrow increases progressively on T1-weighted MRI, reflecting the progressive increase in fat content. Therefore, marrow SI lower than normal muscle almost always indicates pathology.

Spinal bone marrow is characterized by the presence of red marrow throughout life, but the proportions of red and yellow marrow in the axial skeleton vary by age and environmental factors. Women have a larger amount of hematopoietic marrow in early adulthood, with a decline in the water-fat fraction after 60 years compared with men, in whom the decline is in the first 25 years [36]. Red marrow tends to be diffuse in the axial bone marrow under the age of 40 years with only small areas of yellow marrow around the basivertebral plexus [68]. Within individual bones, red marrow is often symmetric [4, 9]. With advancing age, generally over age 40 years, the vertebral bone marrow becomes increasingly replaced with fatty marrow. This may occur in one of three patterns: a bandlike pattern of fatty replacement along the endplates, small foci of fatty marrow replacement, or larger globular areas of fat replacement [68] (Fig. 12). Some elderly patients and patients with malnutrition or osteoporosis may have near-complete replacement of vertebral marrow by fat [47, 48].

The bone marrow is a dynamic organ that undergoes changes both during development and, due to the extensive vascularity of bone marrow, in relatively rapid response to changes in environmental factors, including dietary changes, anemia, chronic hypoxia, chemotherapy, and other medications, through various cytokines [69, 70]. Chronic smoking may result in tissue hypoxia because of elevated carboxyhemoglobin levels [71], and long-distance running can lead to anemia from chronic mechanical hemolysis [72]. In pregnancy, there may be folate deficiency related to rapid cell turnover with development of megaloblastic anemia [73] (Fig. 13). The bone marrow of such patients may show benign hematopoietic hyperplasia with patchy areas of T1 hypointensity. Patients with sickle cell disease or other chronic diseases that stress the bone marrow will tend to reconvert the yellow marrow to red marrow or may never convert the red marrow to yellow marrow. This adaptive nature of bone marrow must be kept in mind when reviewing spinal MRI.

References

1. Vande Berg BC, Malgem J, Lecouvet FE, Maldaque B. Magnetic resonance imaging of normal bone marrow. *Eur Radiol* 1998; 8:1327–1334
2. Vogler JB 3rd, Murphy WA. Bone marrow imaging. *Radiology* 1988; 168:679–693
3. Vande Berg BC, Malgem J, Lecouvet FE, Maldaque B. Classification and detection of bone marrow lesions with magnetic resonance imaging. *Skeletal Radiol* 1998; 27:529–545
4. Daffner RH, Lupetin AR, Dash N, Deeb ZL, Sefczek RJ, Schapiro RL. MRI in the detection of malignant infiltration of bone marrow. *AJR* 1986; 146:353–358
5. Baur A, Stäbler, Brüning R, et al. Diffusion-weighted MR imaging of bone marrow: differentiation of benign versus pathologic compression fractures. *Radiology* 1998; 207:349–356
6. Carroll KW, Feller JF, Tirman PF. Useful internal standards for distinguishing infiltrative marrow pathology from hematopoietic marrow at MRI. *J Magn Reson Imaging* 1997; 7:394–398
7. Zhao J, Krug R, Xu D, Lu Y, Link TM. MRI of the spine: image quality and normal-neoplastic bone marrow contrast at 3 T versus 1.5 T. *AJR* 2009; 192:873–880
8. Schweitzer ME, Levine C, Mitchell DG, Gannon FH, Gomella LG. Bull's-eyes and halos: useful MR discriminators of osseous metastases. *Radiology* 1993; 188:249–252
9. Levine CD, Schweitzer ME, Ehrlich SM. Pelvic marrow in adults. *Skeletal Radiol* 1994; 23:343–347
10. Mirowitz SA, Apicella P, Reinus WR, Hammerman AM. MR imaging of bone marrow lesions: relative conspicuousness on T1-weighted, fat-suppressed T2-weighted, and STIR images. *AJR* 1994; 162:215–221
11. Haubold-Reuter BG, Duewell S, Schilcher BR, Marincek B, von Schulthess GK. The value of bone scintigraphy, bone marrow scintigraphy and fast spin-echo magnetic resonance imaging in staging of patients with malignant solid tumours: a prospective study. *Eur J Nucl Med* 1993; 20:1063–1069
12. Jones KM, Unger EC, Granstrom P, Seeger JF, Carmody RE, Yoshino M. Bone marrow imaging using STIR at 0.5 and 1.5 T. *Magn Reson Imaging* 1992; 10:169–176
13. Gerdes CM, Kijowski R, Reeder SB. IDEAL imaging of the musculoskeletal system: robust water fat separation for uniform fat suppression, marrow evaluation, and cartilage imaging. *AJR* 2007; 189:1198; [web]W284–W291
14. Uchida N, Sugimura K, Kajitani A, Yoshizako T, Ishida T. MR imaging of vertebral metastases:

evaluation of fat saturation imaging. *Eur J Radiol* 1993; 17:91–94

15. Bydder GM, Steiner RE, Blumgart LH, Khenia S, Young IR. MR imaging of the liver using short TI inversion recovery sequences. *J Comput Assist Tomogr* 1985; 9:1084–1089
16. Kellenberger CJ, Epelman M, Miller SF, Babyn PS. Fast STIR whole-body MR imaging in children. *RadioGraphics* 2004; 24:1317–1330
17. Rahmouni A, Divine M, Mathieu D, et al. Detection of multiple myeloma involving the spine: efficacy of fat-suppression and contrast-enhanced MR imaging. *AJR* 1993; 160:1049–1052
18. Georgy BA, Hesselink JR, Middleton MS. Quantitative analysis of signal intensities and contrast after fat suppression in contrast-enhanced magnetic resonance imaging of the spine. *Acad Radiol* 1996; 3:731–734
19. Meyer JS, Siegel JS, Faroogul SO, Jaramillo D, Fletcher BD, Hoffer FA. Which MRI sequence of the spine best reveals bone-marrow metastases of neuroblastoma? *Pediatr Radiol* 2005; 35:778–785
20. Georgy BA, Hesselink JR. Evaluation of fat suppression in contrast-enhanced MR of neoplastic and inflammatory spine disease. *AJNR* 1994; 15:409–417
21. Carmody RF, Yang PJ, Seeley GW, Seeger JF, Unger EC, Johnson JE. Spinal cord compression due to metastatic disease: diagnosis with MR imaging versus myelography. *Radiology* 1989; 173:225–229
22. Hajnal JV, Bryant DJ, Kasuboski L, et al. Use of fluid attenuated inversion recovery (FLAIR) pulse sequences in MRI of the brain. *J Comput Assist Tomogr* 1992; 16:841–844
23. White SJ, Hajnal JV, Young IR, Bydder GM. Use of fluid-attenuated inversion-recovery pulse sequences for imaging the spinal cord. *Magn Reson Med* 1992; 28:153–162
24. Phalke VV, Gujar S, Quint DJ. Comparison of 3.0 T versus 1.5 T MR: imaging of the spine. *Neuroimaging Clin N Am* 2006; 16:241–248
25. Shapiro MD. MR imaging of the spine at 3T. *Magn Reson Imaging Clin N Am* 2006; 14:97–108
26. Rydberg JN, Hammond CA, Grimm RC, et al. Initial clinical experience in MR imaging of the brain with a fast fluid-attenuated inversion-recovery pulse sequence. *Radiology* 1994; 193:173–180
27. Rydberg JN, Hammond CA, Huston J 3rd, Jack CR Jr, Grimm RC, Riederer SJ. T1-weighted MR imaging of the brain using a fast inversion recovery pulse sequence. *J Magn Reson Imaging* 1996; 6:356–362
28. Melhem ER, Israel DA, Eustace S, Jara H. MR of the spine with a fast T1-weighted fluid-attenuated inversion recovery sequence. *AJNR* 1997; 18:447–454
29. Lavdas E, Vlychou M, Arikidis N, Kapsalaki E, Roca V, Fezoulidis IV. Comparison of T1-weighted fast spin-echo and T1-weighted fluid-attenuated inversion recovery images of the lumbar spine at 3.0 Tesla. *Acta Radiol* 2010; 51:290–295
30. Castillo M, Arbelaez A, Smith JR, Fisher LL. Diffusion-weighted MR imaging offers no advantage over routine noncontrast MR imaging in the detection of vertebral metastases. *AJNR* 2000; 21:948–953
31. Herneth AM, Naude J, Philipp M, Beichel R, Trattnig S, Imhof H. The value of diffusion-weighted MRT in assessing the bone marrow changes in vertebral metastases [in German]. *Radiologe* 2000; 40:731–736
32. Plank C, Koller A, Nueller-Mang C, Bammer R, Thurnher MM. Diffusion-weighted MR imaging (DWI) in the evaluation of epidural spinal lesions. *Neuroradiology* 2007; 49:977–985
33. Eguchi Y, Ohtori S, Yamashita M, et al. Diffusion magnetic resonance imaging to differentiate degenerative from infectious endplate abnormalities in the lumbar spine. *Spine* 2011; 36:E198–E202
34. Hanna SL, Fletcher BD, Fairclough DL, Jenkins JH 3rd, Le AH. Magnetic resonance imaging of disseminated bone marrow disease in patients treated for malignancy. *Skeletal Radiol* 1991; 20:79–84
35. Byun WM, Shin SO, Chany Y, Lee SJ, Finsterbusch J, Frahm J. Diffusion-weighted MR imaging of metastatic disease of the spine: assessment of response to therapy. *AJNR* 2002; 23:906–912
36. Ishijima H, Ishizaka H, Horikoshi H, Sakurai M. Water fraction of lumbar vertebral bone marrow estimated from chemical shift misregistration on MR imaging: normal variations with age and sex. *AJR* 1996; 167:355–358
37. Gokalp G, Mutlu FS, Yazici Z, Yildrim N. Evaluation of vertebral bone marrow fat content by chemical-shift MRI in osteoporosis. *Skeletal Radiol* 2011; 40:577–585
38. Wismer GL, Rosen BR, Buxton R, Stark DD, Brady TJ. Chemical shift imaging of bone marrow: preliminary experience. *AJR* 1985; 145:1031–1037
39. Swartz PG, Roberts CC. Radiological reasoning: bone marrow changes on MRI. *AJR* 2009; 193(3 suppl):S1–S4; quiz, S5–S9
40. Disler DG, McCauley TR, Ratner LM, Kesack CD, Cooper JA. In-phase and out-of-phase MR imaging of bone marrow: prediction of neoplasia based on the detection of coexistent fat and water. *AJR* 1997; 169:1439–1447
41. Erly WK, Oh ES, Outwater EK. The utility of in-phase/opposed-phase imaging in differentiating malignancy from acute benign compression fractures of the spine. *AJNR* 2006; 27:1183–1188
42. Ragab Y, Emad Y, Gheita T, et al. Differentiation of osteoporotic and neoplastic vertebral fractures by chemical shift (in-phase and out-of-phase) MR imaging. *Eur J Radiol* 2009; 72:125–133
43. Saifuddin A, Bann K, Ridgeway JP, Butt WP. Bone marrow blood supply in gadolinium-enhanced magnetic resonance imaging. *Skeletal Radiol* 1994; 23:455–457
44. Baur A, Stabler A, Bartl R, Lamerz R, Sheidler J, Reiser M. MRI gadolinium enhancement of bone marrow: age-related changes in normals and in diffuse neoplastic infiltration. *Skeletal Radiol* 1997; 26:414–418
45. Montazel JL, Divine M, Lepage E, Kobeiter H, Breil S, Rahmouni A. Normal spinal bone marrow in adults: dynamic gadolinium-enhanced MR imaging. *Radiology* 2003; 229:703–709
46. Chen WT, Shih TT, Chen RC, et al. Vertebral bone marrow perfusion evaluated with dynamic contrast-enhanced MR imaging: significance of aging and sex. *Radiology* 2001; 220:213–218
47. Griffith JF, Yeung DK, Antonio GE, et al. Vertebral marrow fat content and diffusion and perfusion indexes in women with varying bone density: MR evaluation. *Radiology* 2006; 241:831–838
48. Griffith JF, Yeung DK, Antonio GE, et al. Vertebral bone mineral density, marrow perfusion, and fat content in healthy men and men with osteoporosis: dynamic contrast-enhanced MR imaging and MR spectroscopy. *Radiology* 2005; 236:945–951
49. Rahmouni A, Montazel JL, Divine M, et al. Bone marrow with diffuse tumor infiltration in patients with lymphoproliferative diseases: dynamic gadolinium-enhanced MR imaging. *Radiology* 2003; 229:710–717
50. Nosas-Garcia S, Moehler T, Wasser K, et al. Dynamic contrast-enhanced MRI for assessing the disease activity of multiple myeloma: a comparative study with histology and clinical markers. *J Magn Reson Imaging* 2005; 22:154–162
51. Moulopoulos LA, Maris TG, Papanikolaou N, Panagi G, Vlahos L, Dimopoulos MA. Detection of malignant bone marrow involvement with dynamic contrast-enhanced magnetic resonance imaging. *Ann Oncol* 2003; 14:152–158
52. Kanchiku T, Taguchi T, Toyoda K, Fujii K, Kawai S. Dynamic contrast-enhanced magnetic resonance imaging of osteoporotic vertebral fracture. *Spine* 2003. 28:2522–2526; discussion, 2
53. Maris TG, Damilakis J, Sideri L, et al. Assessment of the skeletal status by MR relaxometry techniques of the lumbar spine: comparison with dual X-ray absorptiometry. *Eur J Radiol* 2004; 50:245–256
54. Schick F, Einsele H, Bongers H, et al. Leukemic red bone marrow changes assessed by magnetic resonance imaging and localized ^{1}H spectroscopy. *Ann Hematol* 1993; 66:3–13
55. Schick F, Seitz D, Machann J, Lutz O, Claussen CD. Magnetic resonance bone densitometry: comparison of different methods based on susceptibility. *Invest Radiol* 1995; 30:254–265
56. Schick F, Bongers H, Jung WI, Skalai M, Lutz O,

Claussen CD. Volume-selective proton MRS in vertebral bodies. *Magn Reson Med* 1992; 26:207–217
57. Brix G, Heiland S, Bellemann ME, Koch T, Lorenz WJ. MR imaging of fat-containing tissues: valuation of two quantitative imaging techniques in comparison with localized proton spectroscopy. *Magn Reson Imaging* 1993; 11:977–991
58. Schellinger D, Lin CS, Hatipaglu HG, Fertikh D. Potential value of vertebral proton MR spectroscopy in determining bone weakness. *AJNR* 2001; 22:1620–1627
59. Schellinger D, Lin CS, Fertikh D, et al. Normal lumbar vertebrae: anatomic, age, and sex variance in subjects at proton MR spectroscopy—initial experience. *Radiology* 2000; 215:910–916
60. Demmler K, Burkhardt R. Relations between fatty tissue, cancellous bone and vascular pattern of the iliac bone in aplastic anaemia. *Bibl Haematol* 1978; 45:109–117
61. Luypaert R, Bouiraf S, Sourbron S, Osteaux M. Diffusion and perfusion MRI: basic physics. *Eur J Radiol* 2001; 38:19–27
62. Liu Y, Tang GY, Tang RB, Peng YF, Li W. Assessment of bone marrow changes in postmenopausal women with varying bone densities: magnetic resonance spectroscopy and diffusion magnetic resonance imaging. *Chin Med J (Engl)* 2010; 123:1524–1527
63. Nagae-Poetscher LM, Jiang H, Wakana S, Golay X, van Zil PC, Mori S. High-resolution diffusion tensor imaging of the brain stem at 3 T. *AJNR* 2004; 25:1325–1330
64. Gold GE, Suh B, Sawyer-Glover A, Beaulieu C. Musculoskeletal MRI at 3.0 T: initial clinical experience. *AJR* 2004; 183:1479–1486
65. Vande Berg BC, Lecouvet FE, Galant C, Simoni P, Malhgem J. Normal variants of the bone marrow at MR imaging of the spine. *Semin Musculoskelet Radiol* 2009; 13:87–96
66. Weinreb JC. MR imaging of bone marrow: a map could help. *Radiology* 1990; 177:23–24
67. Vande Berg BC, Lecouvet FE, Michaux L, Ferrant A, Maldaque B, Malghem J. Magnetic resonance imaging of the bone marrow in hematological malignancies. *Eur Radiol* 1998; 8:1335–1344
68. Ricci C, Cova M, Kang YS, et al. Normal age-related patterns of cellular and fatty bone marrow distribution in the axial skeleton: MR imaging study. *Radiology* 1990; 177:83–88
69. Kricun ME. Red-yellow marrow conversion: its effect on the location of some solitary bone lesions. *Skeletal Radiol* 1985; 14:10–19
70. Travlos GS. Normal structure, function, and histology of the bone marrow. *Toxicol Pathol* 2006; 34:548–565
71. Poulton TB, Murphey WD, Duerk JL, Chapek CC, Feiglin DH. Bone marrow reconversion in adults who are smokers: MR imaging findings. *AJR* 1993; 161:1217–1221
72. Shellock FG, Morris E, Deutsch AL, Mink JH, Kerr R, Boden SD. Hematopoietic bone marrow hyperplasia: high prevalence on MR images of the knee in asymptomatic marathon runners. *AJR* 1992; 158:335–338
73. Hoffbrand V, Provan D. ABC of clinical haematology: macrocytic anaemias. *BMJ* 1997; 314:430–433

FOR YOUR INFORMATION

The reader's attention is directed to part 2 accompanying this article, titled "MRI of Spinal Bone Marrow: Part 2, T1-Weighted Imaging-Based Differential Diagnosis," which begins on page 1309.

FOR YOUR INFORMATION

The Self-Assessment Module accompanying this article can be accessed via www.ajronline.org at the article link labeled "CME/SAM."

The American Roentgen Ray Society is pleased to present these Self-Assessment Modules (SAMs) as part of its commitment to lifelong learning for radiologists. Each SAM is composed of two journal articles along with questions, solutions, and references, which can be found online. Read each article, then answer the accompanying questions and review the solutions online. After submitting your responses, you'll receive immediate feedback and benchmarking data to enable you to assess your results against your peers.

Continuing medical education (CME) and SAM credits are available in each issue of the *AJR* and are ***free to ARRS members. Not a member?*** Call 1-866-940-2777 (from the U.S. or Canada) or 703-729-3353 to speak to an ARRS membership specialist and begin enjoying the benefits of ARRS membership today!